



## In-Plane Magnetoresistance Obeys Kohler's Rule in the Pseudogap Phase of Cuprate Superconductors

M. K. Chan,<sup>1,\*</sup> M. J. Veit,<sup>1</sup> C. J. Dorow,<sup>1,†</sup> Y. Ge,<sup>1</sup> Y. Li,<sup>1</sup> W. Tabis,<sup>1,2</sup> Y. Tang,<sup>1</sup> X. Zhao,<sup>1,3</sup> N. Barišić,<sup>1,4,5,‡</sup> and M. Greven<sup>1,§</sup>

<sup>1</sup>*School of Physics and Astronomy, University of Minnesota, Minneapolis, Minnesota 55455, USA*

<sup>2</sup>*AGH University of Science and Technology, Faculty of Physics and Applied Computer Science, Al. A. Mickiewicza 30, 30-059 Krakow, Poland*

<sup>3</sup>*State Key Lab of Inorganic Synthesis and Preparative Chemistry, College of Chemistry, Jilin University, Changchun 130012, China*

<sup>4</sup>*Service de Physique de l'Etat Condensé, CEA-DSM-IRAMIS, F 91198 Gif-sur-Yvette, France*

<sup>5</sup>*Institute of Solid State Physics, Vienna University of Technology, 1040 Vienna, Austria*

(Received 19 February 2014; published 21 October 2014)

We report in-plane resistivity ( $\rho$ ) and transverse magnetoresistance (MR) measurements for underdoped HgBa<sub>2</sub>CuO<sub>4+ $\delta$</sub>  (Hg1201). Contrary to the long-standing view that Kohler's rule is strongly violated in underdoped cuprates, we find that it is in fact satisfied in the pseudogap phase of Hg1201. The transverse MR shows a quadratic field dependence,  $\delta\rho/\rho_0 = aH^2$ , with  $a(T) \propto T^{-4}$ . In combination with the observed  $\rho \propto T^2$  dependence, this is consistent with a single Fermi-liquid quasiparticle scattering rate. We show that this behavior is typically masked in cuprates with lower structural symmetry or strong disorder effects.

DOI: 10.1103/PhysRevLett.113.177005

PACS numbers: 74.72.Kf, 74.25.fc, 74.72.Gh

The unusual metallic “normal state” of the cuprates has remained an enigma. Atypical observations at odds with Fermi-liquid theory have been made particularly in the so-called strange-metal regime above the pseudogap (PG) temperature  $T^*$  [inset of Fig. 1(b)] [1]. In this regime, the in-plane resistivity exhibits an anomalous extended linear temperature dependence,  $\rho \propto T$  [2], and the Hall effect is often described as  $R_H \propto 1/T$  [3,4]. In order to account for this anomalous behavior without abandoning a Fermi-liquid formalism, some descriptions have been formulated based on a scattering rate whose magnitude varies around the in-plane Fermi surface, for example, due to anisotropic umklapp scattering or coupling to a bosonic mode [1] (e.g., spin [5] or charge [6] fluctuations). Prominent non-Fermi-liquid prescriptions, such as the two-lifetime picture [7] and the marginal-Fermi liquid [8], have also been put forth. The former implies charge-spin separation while the latter is a signature of a proximate quantum critical point.

The transport behavior in the PG state ( $T < T^*$ ) has furthermore been complicated not only because of the opening of the PG along portions of the Fermi surface, but also due to possible superconducting (SC) [10], antiferromagnetic [5,11] and charge-spin stripe fluctuations [12].

Recent developments, however, suggest that  $T^*$  marks a phase transition [13] into a state with broken time-reversal symmetry [14,15]. Additionally, the measurable extent of SC fluctuations is likely limited to only a rather small temperature range ( $\approx 30$  K) above  $T_c$  [16,17]. These strong indications that the PG regime is indeed a distinct phase calls for a clear description of its intrinsic properties. In fact, a simple  $\rho = A_2 T^2$  dependence was recently

reported for underdoped HgBa<sub>2</sub>CuO<sub>4+ $\delta$</sub>  (Hg1201) [9]. It was also found that this Fermi-liquid-like behavior appears below a characteristic temperature  $T^{**}$  [ $T_c < T^{**} < T^*$ ; inset of Fig. 1(b)] and that the coefficient  $A_2$  per CuO<sub>2</sub>

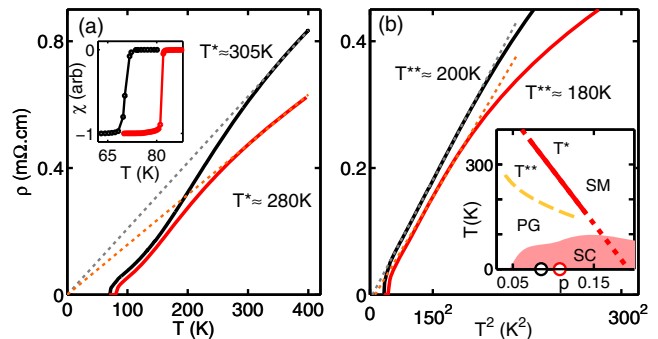


FIG. 1 (color online). (a) Temperature dependence of the in-plane resistivity for two Hg1201 samples. Dotted lines are linear fits to the high-temperature behavior. Inset: Magnetic susceptibility shows  $T_c = 70 \pm 1$  and  $80.5 \pm 0.5$  K for the two samples, HgUD70b (black) and HgUD81 (red). The  $T_c$  values are defined as the midpoint of the transition, and the uncertainties correspond to 90% of the transition width. (b) Resistivity plotted versus  $T^2$ . Dotted lines are fits to  $\rho = A_2 T^2$ . There is some uncertainty in the conversion to units of  $\rho$  due to difficulties in measuring the exact cleaved sample dimensions [9]. For consistency, we have assumed the same magnitude of  $\rho$  for the two  $T_c = 70$  K samples. Inset: Schematic temperature-hole doping phase diagram. The superconducting (SC), strange metal (SM), and pseudogap (PG) phases as well as the characteristic temperatures  $T^*$  and  $T^{**}$  are indicated. The circles represent the two doping levels of the present study.

sheet, is universal [9]. This indication of Fermi-liquid transport was further supported by optical conductivity measurements that demonstrated an  $\omega^2$  dependence and  $\omega - T$  scaling of the scattering rate [18].

For a conventional metal, the change in isothermal resistivity ( $\delta\rho$ ) in an applied magnetic field ( $H$ ) obeys a functional relation known as Kohler's rule:  $\delta\rho/\rho_0 = F(H/\rho_0)$ , where  $\rho_0$  is the zero-field resistivity at a given temperature [19]. This relation follows from the fact that the magnetic field enters Boltzmann's equation in the combination ( $H\tau$ ) and that  $\rho_0$  is proportional to the scattering rate  $1/\tau$ . In the weak-field limit, most simple metals exhibit a  $H^2$  dependence of the MR, so  $\delta\rho/\rho_0 \propto \tau^2 H^2$ . Therefore, a plot of  $\delta\rho/\rho_0$  versus  $(H/\rho_0)^2$  is expected to collapse to a single temperature-independent curve, if the number of charge carriers is constant. Additionally, the temperature dependence of the scattering rate should not significantly depend on the location along the Fermi surface. This condition is satisfied most easily if there is only a single temperature-dependent scattering rate. A number of situations in which Kohler's rule is violated are discussed further in Ref. [20]. For a Fermi liquid with  $1/\tau \propto T^2$ , Kohler's rule is valid if  $\delta\rho/\rho_0 \propto H^2 T^{-4}$ .

Prior studies of  $\text{La}_{2-x}\text{Sr}_x\text{CuO}_4$  (LSCO) and  $\text{YBa}_2\text{Cu}_3\text{O}_{6+y}$  (YBCO) reported that Kohler's rule is strongly violated in both the PG and strange-metal regimes [21–23]. The implication of these results is that charge transport in the cuprates is not as simple as implied by the recent zero-field dc and optical conductivity work [9,18].

In this Letter, we revisit the seemingly anomalous magnetotransport in the PG phase through in-plane resistivity and magnetoresistance measurements of Hg1201. Hg1201 has a simple tetragonal ( $P4/mmm$ ) crystal structure with one copper-oxygen layer per primitive cell and features the highest  $T_c$  at optimal doping of all single-layer cuprates [24,25]. Together with the availability

of high-quality single crystals [26–30], this makes Hg1201 a particularly interesting compound for transport studies. We demonstrate that Kohler's rule is in fact satisfied in the PG phase of Hg1201, and that the temperature dependences of  $\rho$  and MR in the PG phase are consistent with a Fermi-liquid quasiparticle scattering rate. Importantly, we furthermore demonstrate that Kohler's rule is also valid for YBCO, a result previously obscured by crystal twinning and CuO chains. The situation appears to be more complicated for LSCO, for which we show that only a modified version of Kohler's rule is valid.

The preparation of Hg1201 samples for transport measurements is described in Refs. [26,27]. We present measurements on three samples [31]: two with  $T_c = 70$  K (labeled HgUD70a and HgUD70b; hole doping  $p \approx 0.095$ ) and one with  $T_c = 81$  K (HgUD81;  $p \approx 0.11$ ), where the quoted hole concentrations are based on thermoelectric power measurements [32]. Figure 1(a) shows the temperature dependence of  $\rho$ .  $T^*$  is determined from the deviation from approximate high-temperature linear behavior and agrees with prior reported values [9,15]. The same data are plotted versus  $T^2$  in Fig. 1(b). The  $\rho = A_2 T^2$  behavior is observed between the characteristic temperature  $T^{**}$  and  $\sim T_c + 20$  K. Both the linear and the quadratic dependencies extrapolate to a negligible residual resistivity ( $\rho_{\text{res}} \approx 0$ ), which attests to the high quality of the crystals.

The field dependence of  $\rho$  was measured in static and pulsed magnetic fields (Fig. 2) [33]. The pulsed-field measurements were performed up to 30 T at LNCMI-Toulouse, France, in transverse geometry ( $j\parallel ab, H\parallel c$ ). Positive and negative magnetic field sweeps were performed to establish negligible Hall contribution to the data. For the measurements with low static fields, we explicitly removed Hall contamination by obtaining data for both  $H\parallel c$  and  $H\parallel -c$ . The MR is independent of the

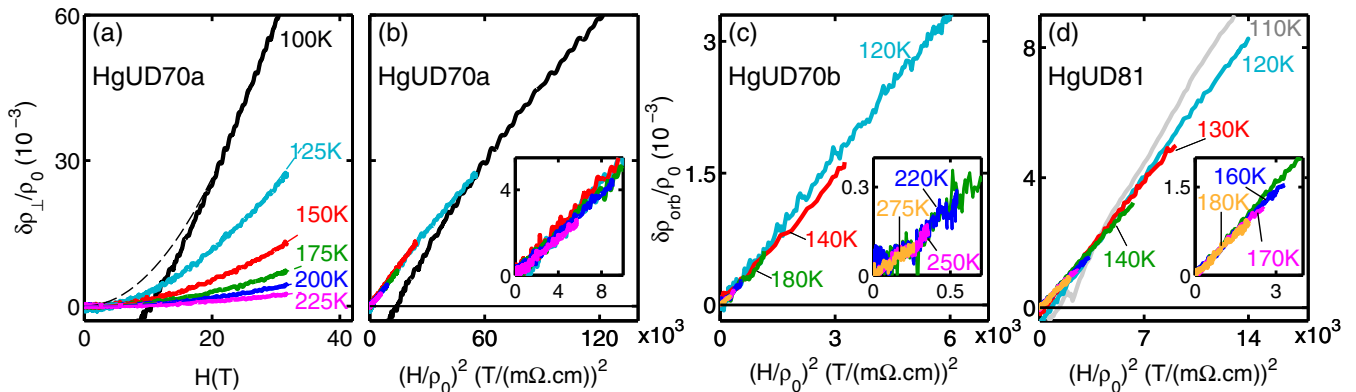


FIG. 2 (color online). (a) Transverse MR with  $H\parallel c$  and  $j\parallel ab$  and (b) the corresponding Kohler plot for sample HgUD70a ( $T_c = 70$  K) measured in a maximum pulsed field of 30 T.  $\rho_0$  is defined as the zero-field resistivity extrapolated from fitting the data above 20 T to the form  $\rho = \rho_0 + a'H^2$ . (c) Kohler plot of the orbital MR [ $\rho(H\parallel c) - \rho(H\parallel j)$ ] with  $j\parallel ab$  for HgUD70b measured in a Quantum Design, Inc. PPMS system up to 9 T. (d) Kohler plot of the orbital MR for HgUD81 measured in fields up to 9 T. Insets to (b)–(d) are low-field views of the respective panels.

magnetic field polarity. The dashed lines in Fig. 2(a) are fits to  $\delta\rho_{\perp}/\rho_0 = a_{\perp}H^2$ , where  $a_{\perp}$  is the transverse MR coefficient. The Kohler plot of the data in Fig. 2(a) is shown in Fig. 2(b). Kohler's rule is satisfied at all fields for temperatures between 125 and 225 K, despite a change in  $\rho_0$  by a factor of  $\sim 6$  in this temperature range. At 100 K, notwithstanding the deviation at low fields, the high-field data (where SC fluctuations [17,34,35] are suppressed, thus revealing the underlying normal state transport) exhibit the same slope.

For YBCO and LSCO, particularly at low doping, a longitudinal MR  $\delta\rho_{\parallel}/\delta\rho_0$  ( $j\parallel ab, H\parallel j$ ) was observed and attributed to an isotropic spin-dependent term [21,36]. This is excluded in the orbital MR defined as  $\delta\rho_{\text{orb}}/\delta\rho_0 \equiv (\delta\rho_{\perp} - \delta\rho_{\parallel})/\rho_0$  [21]. To test the possibility that such contributions might affect our result, we measured the second  $T_c = 70$  K sample (HgUD70b) and established that the longitudinal MR is at least an order of magnitude smaller than the transverse MR. A similarly small longitudinal MR is observed in other cuprates close to optimal doping [23,36]. The orbital MR for HgUD70b is shown in Fig. 2(c). We find that  $\delta\rho_{\text{orb}}/\delta\rho_0$  also satisfies Kohler's rule from 120 to 275 K. Since the longitudinal contribution is small, the transverse and orbital MR

coefficients of HgUD70a and HgUD70b, respectively, are indistinguishable, as shown in Fig. 3(a). Kohler's rule is also found to be obeyed in the PG phase of HgUD81 [Fig. 2(d)]. Our result is therefore not isolated to a particular doping level.

As shown in Fig. 3(a), the MR coefficient ( $a_{\perp, \text{orb}} = \delta\rho_{\perp, \text{orb}}/\rho_0 H^2$ ) exhibits  $T^{-4}$  dependence that extends from approximately 100 K to at least  $T^{**}$ . Since  $\delta\rho/\rho_0 \propto H^2\tau^2 \propto H^2T^{-4}$ , it follows that  $1/\tau \propto T^2$ . For Hg1201, this is consistent with the Fermi-liquid scattering rate below  $T^{**}$  inferred from the temperature dependence of  $\rho$ . The difficulty in measuring the small MR at high temperatures precludes an exact determination of the temperature above which Kohler's rule is violated. If we assume pure  $T^{-4}$  dependence of the MR at all temperatures [21,36], Kohler's rule is violated for  $T > T^{**}$ .

The  $T^{-4}$  dependence of the MR was previously reported for a number of cuprates [4,21,23]. Nevertheless, Kohler's rule was claimed to be violated [4,21–23]. Prior conclusions pertaining to the violation of Kohler's rule in the PG phase of YBCO can be attributed to the difficulty of measuring the underlying pure  $\rho \propto T^2$  behavior. In YBCO, Cu-O chains form along the crystallographic  $b$  direction and contribute to the charge transport, which can prevent a clean measurement of the resistivity of the  $\text{CuO}_2$  planes. Since the relative contribution to  $\rho$  from the chains is temperature dependent, the combined contributions would violate Kohler's rule for twinned crystals reported in Ref. [21]. Measurements of very underdoped nonsuperconducting tetragonal YBCO ( $p \approx 0.03$ ) [4], which does not feature CuO chains, and of the  $a$ -axis resistivity  $\rho_a$  in detwinned YBCO crystals at higher doping [36,38] (the chains are not expected to contribute to transport perpendicular to them) have, in fact, revealed a  $T^2$  resistivity. For example, Fig. 3(b) shows representative data from Ref. [36] with  $T^2$  dependence below a characteristic temperature that decreases with increasing doping, consistent with  $T^{**}$  [9].

As shown in Fig. 3(c), YBCO6.6 exhibits the expected  $a_{\text{orb}} \propto T^{-4}$  dependence of the MR, consistent with the  $\rho = A_2T^2$  dependence and Kohler's rule. In slightly more underdoped YBCO6.5,  $\rho = \rho_{\text{res}} + A_2T^2$  with a large residual resistivity  $\rho_{\text{res}}$ . This is reflected in the MR, which is fit to  $a_{\text{orb}} = (c + bT^2)^{-2}$  [36] [Fig. 3(b)], where  $c$  is a residual temperature independent contribution to the scattering rate. The ratios of the residual term and the  $T^2$  coefficient manifested in the MR ( $c/b = 9700 \text{ K}^2$ ) and in the zero-field resistivity ( $\rho_{\text{res}}/A_2 = 10800 \text{ K}^2$ ) are equivalent to within the uncertainty of the fitted coefficients; thus, Kohler's rule is obeyed as well in YBCO6.5. The temperature dependence of  $\rho$  and the MR in YBCO are consistent with what is found in Hg1201. We conclude that, notwithstanding the significant differences in crystal structures, the normal state of both Hg1201 and YBCO obeys Kohler's rule at temperatures below  $T^{**}$ .

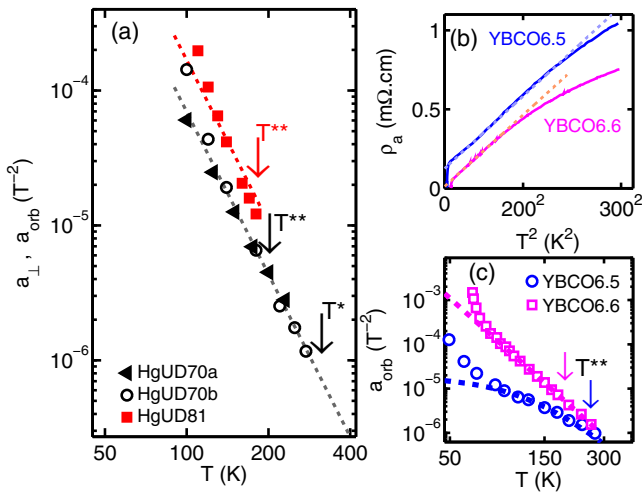


FIG. 3 (color online). (a) Log-log plot of the temperature dependence of the orbital MR coefficient  $a_{\text{orb}} \equiv (a_{\perp} - a_{\parallel})$  for HgUD70b and HgUD81 and of the transverse MR coefficient  $a_{\perp}$  for HgUD70a. The dashed lines are fits to  $a = (bT)^{-4}$ . The arrows mark the characteristic temperatures  $T^*$  and  $T^{**}$ . (b) and (c) show, respectively, representative data for  $a_{\text{orb}}$  and  $a$ -axis in-plane resistivity  $\rho_a$  from Ref. [36] for YBCO6.5 ( $\text{YBa}_2\text{Cu}_3\text{O}_{6+y}$  with  $y = 0.5$ ,  $T_c \approx 35$  K,  $p \approx 0.073$ ) and YBCO6.6 ( $y = 0.6$ ,  $T_c \approx 50$  K,  $p \approx 0.085$ ). We estimate the doping levels by comparing the quoted  $T_c$  values to Ref. [37]. The resistivity in (b) is plotted versus  $T^2$  to highlight the  $\rho_a \propto T^2$  behavior indicated by dashed lines below the characteristic temperature  $T^{**}$ , consistent with the inset of Fig. 1(b). (c) Log-log plot and the dashed lines are fits to the form  $(c + bT^2)^{-2}$ , with  $c = 0$  for YBCO6.6.

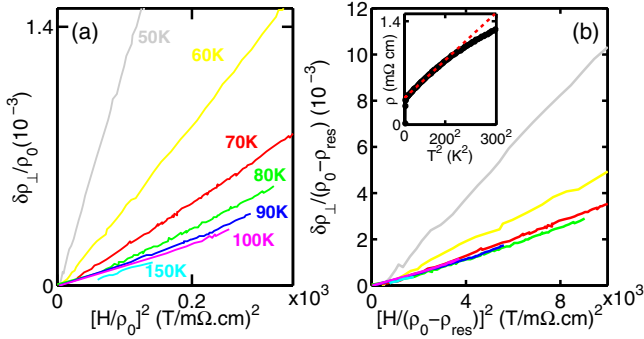


FIG. 4 (color online). (a) Kohler plot for LSCO ( $x = 0.09$ ) from Ref. [23] (b) Modified Kohler plot, with  $\rho_0$  replaced by  $\rho_0 - \rho_{\text{res}}$ . Inset: Temperature dependence of the planar resistivity  $\rho$  in zero field. The dotted red line is a fit to  $\rho = \rho_{\text{res}} + A_2 T^2$ .  $\rho_{\text{res}}$  is determined from extrapolating to  $T = 0$ .

LSCO exhibits some transport properties that are at variance with YBCO and Hg1201: a particularly large residual resistivity and a tendency toward insulating low-temperature behavior [39] below optimal doping, instead of the metallic behavior and quantum oscillations found in YBCO and Hg1201 [29,30,40,41]. LSCO also features lower structural symmetry, more disorder, and a significantly lower optimal  $T_c$  ( $\approx 40$  K) than Hg1201 [24]. Nevertheless, the planar resistivity for moderately underdoped LSCO ( $x = 0.09$ ) is fit well to  $\rho = \rho_{\text{res}} + A_2 T^2$  between 70 and 200 K with a large  $\rho_{\text{res}}$  [inset of Fig. 4(b)] [23]. This is consistent with  $T^{**} \approx 200$  K indicated in Ref. [9]. However, Fig. 4(a) shows the strong violation of Kohler's rule for LSCO. Instead, a modified Kohler's rule, obtained by replacing  $\rho_0$  by  $\rho_0 - \rho_{\text{res}}$ , is obeyed between 70 and 150 K [Fig. 4(b)]. The deviation from this modified Kohler's rule below 70 K might be related to the observation of a large Nernst effect and could be attributed to SC fluctuations [42] or incipient stripe order [43].

The surprising behavior of the MR for LSCO suggests that  $\rho_{\text{res}}$  results not solely from impurity scattering. Indeed, upon decreasing the hole concentration in LSCO, either chemically [44] or through electrostatic gating [45],  $\rho_{\text{res}}$  extrapolated from high temperatures increases progressively upon approaching the superconductor-insulator phase transition. Electrostatic gating revealed a critical  $\text{CuO}_2$  sheet resistance of  $R_c \approx h/(2e)^2 = 6.5$  k $\Omega$  [45]. Similar observations for the superconductor-insulator transition have been made for YBCO [46,47] and  $\text{Bi}_2\text{Sr}_2\text{Y}_x\text{Ca}_{1-x}\text{Cu}_2\text{O}_8$  [48]. Furthermore, for LSCO, a nonzero extrapolated  $\rho_{\text{res}}$  is observed in SC samples up to optimal doping [44], and when the SC is suppressed in a sufficiently large magnetic field, an insulating ground state is revealed [39]. This phenomenon coincides with the presence of nearly static incommensurate spin correlations observed with neutron scattering [49,50]. In contrast,  $\rho_{\text{res}}$  for Hg1201 is small even in the most underdoped single crystals measured ( $p \approx 0.055$ ,  $T_c = 45$  K [9]).

The emerging picture for electrical transport in the underdoped cuprates at temperatures below  $T^{**}$  is that of a Fermi liquid, characterized by a  $T^2$  and  $\omega^2$  [18] quasiparticle scattering rate. Angle-resolved photoemission spectroscopy (ARPES) indicates that a large PG appears in the antinodal density of states below  $T^*$ , leaving small arcs around the nodal points [51]. The Fermi liquid must therefore reside on the arcs [4,9,38,52], where quasiparticle peaks have been detected with ARPES [53]. Upon warming above  $T^{**}$ , the resistivity deviates from the simple quadratic temperature dependence. Whether or not  $T^{**}$  is a true phase transition or merely a crossover temperature, possibly marking the temperature below which the pseudogap is fully formed, is an open question.

One consequence of the validity of Kohler's rule demonstrated in the present work is that the Fermi surface should remain largely temperature independent between  $T^{**}$  and  $T_c + 20$  K. Charge-density-wave (CDW) correlations have been observed in underdoped YBCO [54,55], and also recently in Hg1201 at the same hole concentration as the HgUD70 samples studied here [56]. Interestingly, these correlations in both Hg1201 and YBCO appear at or below  $T^{**}$  [56]. The Fermi-liquid regime below  $T^{**}$  extends to very low hole concentrations [9], in contrast to the CDW order, which appears to be tied to the doping range of the  $T_c(p)$  plateau [54]. Moreover, resistivity [9] and ARPES [57] results suggest the existence of an arclike surface with a doping-independent Fermi velocity. The appearance of CDW correlations might therefore be contingent on the stable Fermi surface below  $T^{**}$  suggested by the present work. ARPES results do indicate that the arc length remains constant over a wide temperature range in the PG regime of  $(\text{Bi}, \text{Pb})_2 \times (\text{Sr}, \text{La})_2\text{CuO}_{6+\delta}$  (Bi2201) and  $\text{Bi}_2\text{Sr}_2\text{CaCu}_2\text{O}_{8+\delta}$  (Bi2212) near optimal doping [58]. However, a complication with Bi2201 and Bi2212 is that zero-field transport does not yield the underlying Fermi-liquid charge transport [9]. It has recently been demonstrated for optimally doped Hg1201 that quantitative ARPES measurements are feasible for this cuprate [59], and it would be interesting to extend such measurements to lower doping.

We thank C. Proust and B. Vignolle for technical assistance in performing the pulsed field measurements at LNCMI-Toulouse, France. We also acknowledge technical assistance by Jan Jaroszynski at the NHMFL, Tallahassee, FL, USA, while performing high static field measurements. The work at the University of Minnesota was supported by the Department of Energy, Office of Basic Energy Sciences, under Award No. DE-SC0006858. The work in Toulouse was supported by the French ANR SUPERFIELD, Euromagnet II, and the LABEX NEXT. N. B. acknowledges support from a Marie Curie Fellowship through the European Commission and from the European Research Council (Advanced Grant Quantum Puzzle, No. 227378).

- \*mchan@physics.umn.edu  
 †Present address: Department of Physics, University of California, San Diego, 9500 Gilman Drive La Jolla, CA 92093, USA.  
 ‡barisic@ifp.tuwien.ac.at  
 §greven@physics.umn.edu
- [1] N. E. Hussey, *J. Phys. Condens. Matter* **20**, 123201 (2008).  
 [2] S. Martin, A. T. Fiory, R. M. Fleming, L. F. Schneemeyer, and J. V. Wazczak, *Phys. Rev. B* **41**, 846 (1990).  
 [3] H. Y. Hwang, B. Batlogg, H. Takagi, H. L. Kao, J. Kwo, R. J. Cava, J. J. Krajewski, and W. F. Peck, Jr., *Phys. Rev. Lett.* **72**, 2636 (1994).  
 [4] Y. Ando, Y. Kurita, S. Komiyama, S. Ono, and K. Segawa, *Phys. Rev. Lett.* **92**, 197001 (2004).  
 [5] P. Monthoux and D. Pines, *Phys. Rev. B* **49**, 4261 (1994).  
 [6] C. Castellani, C. Di Castro, and M. Grilli, *Phys. Rev. Lett.* **75**, 4650 (1995).  
 [7] P. W. Anderson, *Phys. Rev. Lett.* **67**, 2092 (1991).  
 [8] C. M. Varma, P. B. Littlewood, S. Schmitt-Rink, E. Abrahams, and A. E. Ruckenstein, *Phys. Rev. Lett.* **63**, 1996 (1989).  
 [9] N. Barišić, M. K. Chan, Y. Li, G. Yu, X. Zhao, M. Dressel, A. Smontara, and M. Greven, *Proc. Natl. Acad. Sci. U.S.A.* **110**, 12 235 (2013).  
 [10] Z. A. Xu, N. P. Ong, Y. Wang, T. Kakeshita, and S. Uchida, *Nature (London)* **406**, 486 (2000); V. J. Emery and S. A. Kivelson, *Nature (London)* **374**, 434 (1995).  
 [11] B. Batlogg and V. J. Emery, *Nature (London)* **382**, 20 (1996).  
 [12] V. J. Emery, S. A. Kivelson, and O. Zachar, *Phys. Rev. B* **56**, 6120 (1997).  
 [13] A. Shekhter, B. J. Ramshaw, R. Liang, W. N. Hardy, D. A. Bonn, F. F. Balakirev, R. D. McDonald, J. B. Betts, S. C. Riggs, and A. Migliori, *Nature (London)* **498**, 75 (2013).  
 [14] B. Fauqué, Y. Sidis, V. Hinkov, S. Pailhès, C. T. Lin, X. Chaud, and P. Bourges, *Phys. Rev. Lett.* **96**, 197001 (2006).  
 [15] Y. Li, V. Balédent, N. Barišić, Y. Cho, B. Fauqué, Y. Sidis, G. Yu, X. Zhao, P. Bourges, and M. Greven, *Nature (London)* **455**, 372 (2008); Y. Li, V. Balédent, N. Barišić, Y. C. Cho, Y. Sidis, G. Yu, X. Zhao, P. Bourges, and M. Greven, *Phys. Rev. B* **84**, 224508 (2011).  
 [16] M. S. Grbić, N. Barišić, A. Dulčić, I. Kupčić, Y. Li, X. Zhao, G. Yu, M. Dressel, M. Greven, and M. Požek, *Phys. Rev. B* **80**, 094511 (2009); L. S. Bilbro, R. V. Aguilar, G. Logvenov, O. Pelleg, I. Božović, and N. P. Armitage, *Nat. Phys.* **7**, 298 (2011); M. S. Grbić, M. Požek, D. Paar, V. Hinkov, M. Raichle, D. Haug, B. Keimer, N. Barišić, and A. Dulčić, *Phys. Rev. B* **83**, 144508 (2011); G. Yu, D. D. Xia, N. Barišić, R. H. He, N. Kaneko, T. Sasagawa, Y. Li, X. Zhao, A. Shekhter, and M. Greven, [arXiv:1210.6942](https://arxiv.org/abs/1210.6942).  
 [17] F. Rullier-Albenque, H. Alloul, C. Proust, P. Lejay, A. Forget, and D. Colson, *Phys. Rev. Lett.* **99**, 027003 (2007).  
 [18] S. Mirzaei, D. Stricker, J. Hancock, C. Berthod, A. Georges, E. van Heumen, M. K. Chan, X. Zhao, Y. Li, M. Greven, N. Barišić, and D. van der Marel, *Proc. Natl. Acad. Sci. U.S.A.* **110**, 5774 (2013).  
 [19] A. P. Pippard, *Magnetoresistance in Metals* (Cambridge University Press, Cambridge, England, 1993).  
 [20] R. H. McKenzie, J. S. Qualls, S. Y. Han, and J. S. Brooks, *Phys. Rev. B* **57**, 11 854 (1998).  
 [21] J. M. Harris, Y. F. Yan, P. Matl, N. P. Ong, P. W. Anderson, T. Kimura, and K. Kitazawa, *Phys. Rev. Lett.* **75**, 1391 (1995).  
 [22] K. Semba and A. Matsuda, *Phys. Rev. B* **55**, 11 103 (1997).  
 [23] T. Kimura, S. Miyasaka, H. Takagi, K. Tamazaki, H. Eisaki, S. Uchida, K. Kitazawa, M. Hiroi, M. Sera, and N. Kobayashi, *Phys. Rev. B* **53**, 8733 (1996).  
 [24] H. Eisaki, N. Kaneko, D. L. Feng, A. Damascelli, P. K. Mang, K. M. Shen, Z.-X. Shen, and M. Greven, *Phys. Rev. B* **69**, 064512 (2004).  
 [25] S. N. Putilin, E. V. Antipov, O. Chmaissem, and M. Marezio, *Nature (London)* **362**, 226 (1993).  
 [26] X. Zhao, G. Yu, Y.-C. Cho, G. Chabot-Couture, N. Barišić, P. Bourges, N. Kaneko, Y. Li, L. Lu, E. M. Motoyama, O. P. Vajk, and M. Greven, *Adv. Mater.* **18**, 3243 (2006).  
 [27] N. Barišić, Y. Li, X. Zhao, Y.-C. Cho, G. Chabot-Couture, G. Yu, and M. Greven, *Phys. Rev. B* **78**, 054518 (2008).  
 [28] Y. Li, N. Egetenmeyer, J. L. Gavilano, N. Barišić, and M. Greven, *Phys. Rev. B* **83**, 054507 (2011).  
 [29] N. Barišić, S. Badoux, M. K. Chan, C. Dorow, W. Tabis, B. Vignolle, G. Yu, J. Béard, X. Zhao, C. Proust, and M. Greven, *Nat. Phys.* **9**, 761 (2013).  
 [30] N. Doiron-Leyraud, S. Lepault, O. Cyr-Choinière, B. Vignolle, G. Grissonnanche, F. Laliberté, J. Chang, N. Barišić, M. K. Chan, L. Ji, X. Zhao, Y. Li, M. Greven, C. Proust, and L. Taillefer, *Phys. Rev. X* **3**, 021019 (2013).  
 [31] The samples have a large  $ab$  plane surface. The  $a/b - c$  edges were cleaved resulting in a “matchstick” shaped sample and Au pads were sputtered on the cleaved edges. The sample dimensions were [length  $\times$  width  $\times$  thickness (distance between voltage contacts)]:  $2.2 \times 0.4 \times 0.3 \text{ mm}^3$  (1.4 mm),  $1 \times 0.3 \times 0.3 \text{ mm}^3$  (0.6 mm) for the two  $T_c = 70 \text{ K}$  samples (HgUD70a and HgUD70b, respectively), and  $0.6 \times 0.4 \times 0.3 \text{ mm}^3$  (0.5 mm) for the  $T_c = 81 \text{ K}$  sample. See Supplemental Material at <http://link.aps.org/supplemental/10.1103/PhysRevLett.113.177005> for an optical micrograph of a contacted sample.  
 [32] A. Yamamoto, W.-Z. Hu, and S. Tajima, *Phys. Rev. B* **63**, 024504 (2000).  
 [33] We have recently performed additional magnetotransport measurements on a sample with ( $p \approx 0.095$ ) in static fields up to 30 T at the National High Magnetic Field Laboratory, Tallahassee, FL, USA. The sample’s dimensions are [length  $\times$  width  $\times$  thickness (distance between voltage contacts)]  $2 \times 0.4 \times 0.3 \text{ mm}^3$  (1.4 mm). These measurements are consistent with the results presented here and further confirm the validity of Kohler’s rule from 100 to 230 K in another sample with  $T_c = 70 \text{ K}$ . The magnitude of the MR at 150 K is  $a = 1.4E - 5(T^{-2})$ , comparable that that shown in Fig. 3(a) for HgUD70a,b.  
 [34] R. A. Cooper, Y. Wang, B. Vignolle, O. J. Lipscombe, S. M. Hayden, Y. Tanabe, T. Adachi, Y. Koike, M. Nohara, H. Takagi, C. Proust, and N. E. Hussey, *Science* **323**, 603 (2009).  
 [35] I. Kokanović, J. R. Cooper, S. H. Naqib, R. S. Islam, and R. A. Chakalov, *Phys. Rev. B* **73**, 184509 (2006).  
 [36] Y. Ando and K. Segawa, *Phys. Rev. Lett.* **88**, 167005 (2002).  
 [37] R. Liang, D. A. Bonn, and W. N. Hardy, *Phys. Rev. B* **73**, 180505 (2006).

- [38] Y. S. Lee, K. Segawa, Z. Q. Li, W. J. Padilla, M. Dumm, S. V. Dordevic, C. C. Homes, Y. Ando, and D. N. Basov, *Phys. Rev. B* **72**, 054529 (2005).
- [39] G. S. Boebinger, Y. Ando, A. Passner, T. Kimura, M. Okuya, J. Shimoyama, K. Kishio, K. Tamasaku, N. Ichikawa, and S. Uchida, *Phys. Rev. Lett.* **77**, 5417 (1996).
- [40] N. Doiron-Leyraud, C. Proust, D. LeBoeuf, J. Levallois, J. Bonnemaïson, R. Liang, D. A. Bonn, W. N. Hardy, and L. Taillefer, *Nature (London)* **447**, 565 (2007).
- [41] D. LeBoeuf, N. Doiron-Leyraud, B. Vignolle, M. Sutherland, B. J. Ramshaw, J. Levallois, R. Daou, F. Laliberté, O. Cyr-Choinière, J. Chang, Y. J. Jo, L. Balicas, R. Liang, D. A. Bonn, W. N. Hardy, C. Proust, and L. Taillefer, *Phys. Rev. B* **83**, 054506 (2011).
- [42] Y. Wang, L. Li, and N. P. Ong, *Phys. Rev. B* **73**, 024510 (2006).
- [43] O. Cyr-Choinière, R. Daou, F. Laliberte, D. LeBoeuf, N. Doiron-Leyraud, J. Chang, J.-Q. Yan, J.-G. Cheng, J.-S. Zhou, J. B. Goodenough, S. Pyon, T. Takayama, H. Takagi, Y. Tanaka, and L. Taillefer, *Nature (London)* **458**, 743 (2009).
- [44] Y. Ando, S. Komiya, K. Segawa, S. Ono, and Y. Kurita, *Phys. Rev. Lett.* **93**, 267001 (2004).
- [45] A. T. Bollinger, G. Dubuis, J. Yoon, D. Pavuna, J. Misewich, and I. Božović, *Nature (London)* **472**, 458 (2011).
- [46] D. J. C. Walker, A. P. Mackenzie, and J. R. Cooper, *Phys. Rev. B* **51**, 15653 (1995).
- [47] X. Leng, J. Garcia-Barriocanal, S. Bose, Y. Lee, and A. M. Goldman, *Phys. Rev. Lett.* **107**, 027001 (2011).
- [48] D. Mandrus, L. Forro, C. Kendziora, and L. Mihaly, *Phys. Rev. B* **44**, 2418 (1991).
- [49] K. Yamada, C. H. Lee, K. Kurahashi, J. Wada, S. Wakimoto, S. Ueki, H. Kimura, Y. Endoh, S. Hosoya, G. Shirane, R. J. Birgeneau, M. Greven, M. A. Kastner, and Y. J. Kim, *Phys. Rev. B* **57**, 6165 (1998).
- [50] M. Kofu, S.-H. Lee, M. Fujita, H.-J. Kang, H. Eisaki, and K. Yamada, *Phys. Rev. Lett.* **102**, 047001 (2009).
- [51] A. Damascelli, Z. Hussain, and Z. Shen, *Rev. Mod. Phys.* **75**, 473 (2003).
- [52] L. P. Gor'kov, *Phys. Rev. B* **88**, 041104 (2013).
- [53] T. Yoshida, X. J. Zhou, T. Sasagawa, W. L. Yang, P. V. Bogdanov, A. Lanzara, Z. Hussain, T. Mizokawa, A. Fujimori, H. Eisaki, Z. X. Shen, T. Kakeshita, and S. Uchida, *Phys. Rev. Lett.* **91**, 027001 (2003).
- [54] G. Ghiringhelli, M. LeTacon, M. Minola, S. Blanco-Canosa, C. Mazzoli, N. B. Brookes, G. M. D. Luca, A. Frano, D. G. Hawthorn, F. He, T. Loew, M. M. Sala, D. C. Peets, M. Salluzzo, E. Schierle, R. Sutarto, G. A. Sawatzky, E. Weschke, B. Keimer, and L. Braicovich, *Science* **337**, 821 (2012).
- [55] J. Chang, E. Blackburn, A. T. Holmes, N. B. Christensen, J. Larsen, J. Mesot, R. Liang, D. A. Bonn, W. N. Hardy, A. Watenphul, M. Zimmermann, E. M. Forgan, and S. M. Hayden, *Nat. Phys.* **8**, 871 (2011).
- [56] W. Tabis, Y. Li, M. LeTacon, L. Braicovich, A. Kreyssig, M. Minola, G. Dellea, E. Weschke, M. J. Veit, A. I. Goldman, T. Schmitt, G. Ghiringhelli, N. Barišić, M. K. Chan, C. J. Dorow, G. Yu, X. Zhao, B. Keimer, and M. Greven, *arXiv:1404.7658*.
- [57] X. J. Zhou *et al.*, *Nature (London)* **423**, 398 (2003).
- [58] T. Kondo, A. D. Palczewski, Y. Hamaya, T. Takeuchi, J. S. Wen, Z. J. Xu, G. Gu, and A. Kaminski, *Phys. Rev. Lett.* **111**, 157003 (2013).
- [59] I. M. Vishik, N. Barišić, M. K. Chan, Y. Li, D. D. Xia, G. Yu, X. Zhao, W. S. Lee, W. Meevasana, T. P. Devereaux, M. Greven, and Z. X. Shen, *Phys. Rev. B* **89**, 195141 (2014).